

Symmetrical Analysis of a Six-Phase Induction Machine Under Fault Conditions

E. K. Appiah, G. M'boungui, A. A. Jimoh, J. L. Munda, and A.S.O. Ogunjuyigbe

Abstract—The operational behavior of a six-phase squirrel cage induction machine with faulted stator terminals is presented in this paper. The study is carried out using the derived mathematical model of the machine in the arbitrary reference frame. Tests are conducted on a 1 kW experimental machine.

Steady-state and dynamic performance are analyzed for the machine unloaded and loaded conditions. The results shows that with one of the stator phases experiencing either an open- circuit or short circuit fault the machine still produces starting torque, albeit the running performance is significantly derated.

Keywords—Performance, fault conditions, six-phase induction machine.

I. INTRODUCTION

INDUCTION machines can be seen as a standard for industrial electrical alternating current (AC) drives. They are the workhorses of today's industry because as motors they indeed present several advantages such as relatively low cost, reliability, robustness and very little maintenance. They can also be used in hazardous environments such as mining, blowing and pumping operations [1], [2].

Research done over the last three decades showed the advantages of using induction machines with a higher phase order [3]. They can operate with an asymmetrical winding structure in the case of loss of one or more inverter legs or machine phases thus making them fault tolerant [4]. The machines are also used in high-power/high-current applications: for example in electric ship propulsion, locomotive traction and in electric/hybrid electric vehicles [2].

Some research findings have been reported in literature on the fault analysis of three and six phase induction machines. The fault analyses of symmetrical and dynamic simulations of three phase induction machines are detailed in [5] and [6]. It turns out that the developed methods cannot be directly and effectively applied to the analysis of a six phase symmetrical

machine. That is why [13] suggesting that the way to deal with the analysis of the 6 phase machine is rather for example to extend the methods originally developed for the 3 phase machines. Singh *et al* investigated the performance of a faulty six-phase induction machine with an asymmetrical winding [7]. But, investigating single phasing which is in fact a condition in which the motor operates with one phase in open circuit, the authors only considered the case of a momentary fault occurrence. However in the field of multi-phase induction machines Lipo used two separate models for balanced and unbalanced conditions in the analysis of an open circuit fault [8]. Finally, a study was conducted on the modeling and analysis of the symmetrical six-phase induction machine under fault. The machine was supplied through an inverter using Pulse Width Modulation (PWM), which it is known contains a distorted current due to the carrier frequency that increases the copper losses in the motor windings [12], and the authors resorted to a mathematical model in which currents are the state variables [9].

None of the work mentioned above on six-phase machines made apparent the performance of the machine in loaded and unloaded conditions.

This paper presents the performance analysis and simulations of a symmetrical six phase induction machine with 60° displacements between stator windings. A detailed transient and steady state analysis of the machine under fault both in the loaded and unloaded conditions is provided thanks to the use of a known model [9] conveniently adapted to the study with flux linkages as state variables. This model is initially described and validated before starting the inherent performance analysis. Furthermore, in single phasing, the study considers not only leaving the affected phase open-circuited briefly like in number of studies such as [7] but leaving the faulty phase continually open so as to simulate the result of one of the supply fuses being blown as it often occurs in practice.

II. MODELING OF THE MACHINE

Fig. 1 shows the symmetrical six phase induction machine diagram with the stator displaced at 60° between the phases.

E.K. Appiah is a student with Department of Electrical Engineering, Private Bag X680, Pretoria 0001, Republic of South Africa (e-mail: edusam2003@yahoo.com).

G. M'boungui is a post-doctoral fellow with Department of Electrical Engineering, Private Bag X680, Pretoria 0001, Republic of South Africa (e-mail: mboungui@yahoo.fr).

A. A. Jimoh is a Professor with Department of Electrical Engineering, Private Bag X680, Pretoria 0001, Republic of South Africa (e-mail: jimohaa@tut.ac.za).

J. L. Munda is a Professor with Department of Electrical Engineering, Private Bag X680, Pretoria 0001, Republic of South Africa (e-mail: mundajl@tut.ac.za).

A.S.O. Ogunjuyigbe is a Lecturer with Electrical & Electronic Engineering Department, University of Ibadan, Ibadan.

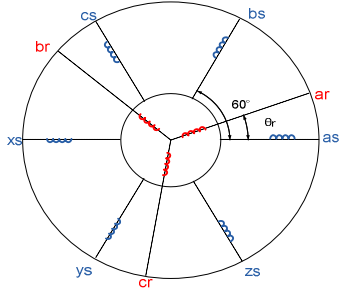


Fig. 1 Machine Diagram in natural reference frame

The cage rotor is represented as a three phase system and is displaced by 120° between the phases.

The voltage equations in the natural reference frame may be expressed as:

$$v_{abcxyzs} = i_{abcxyzs} r_s + \frac{d}{dt} \lambda_{abcxyzs} \quad (1)$$

$$v_{abcr} = i_{abcr} r_r + \frac{d}{dt} \lambda_{abcr} \quad (2)$$

where v the voltage and i the current. The subscripts s and r respectively denote the stator and rotor while r_s and r_r are diagonal matrices of stator and rotor resistances respectively.

The general voltage equation from the natural reference frame to the d - q - θ reference frame is described in [6] [10]. Applied to the six phase case as in [11], the symmetrical α - β voltage equation with flux linkage as state variables are expressed as:

$$V_{ds} = r_s \left(\frac{\lambda_{ds} - \lambda_{md}}{l_s} \right) + \frac{d}{dt} \lambda_{ds} - \omega \lambda_{qs} \quad (3)$$

$$V_{qs} = r_s \left(\frac{\lambda_{qs} - \lambda_{mq}}{l_s} \right) + \frac{d}{dt} \lambda_{qs} + \omega \lambda_{ds} \quad (4)$$

$$V_{dxs} = r_s \left(\frac{\lambda_{dxs}}{l_s} \right) + \frac{d}{dt} \lambda_{dxs} \quad (5)$$

$$V_{qys} = r_s \left(\frac{\lambda_{qys}}{l_s} \right) + \frac{d}{dt} \lambda_{qys} \quad (6)$$

$$V_{os1} = r_s \left(\frac{\lambda_{os1}}{l_s} \right) + \frac{d}{dt} \lambda_{os1} \quad (7)$$

$$V_{os2} = r_s \left(\frac{\lambda_{os2}}{l_s} \right) + \frac{d}{dt} \lambda_{os2} \quad (8)$$

$$V_{dr} = r_r \left(\frac{\lambda_{dr} - \lambda_{md}}{l_r} \right) + \frac{d}{dt} \lambda_{dr} - (\omega - \omega_r) \lambda_{qr} \quad (9)$$

$$V_{qr} = r_r \left(\frac{\lambda_{qr} - \lambda_{mq}}{l_r} \right) + \frac{d}{dt} \lambda_{qr} + (\omega - \omega_r) \lambda_{dr} \quad (10)$$

The flux linkage equations are also expressed as [11]:

$$\lambda_{ds} = Ll_s i_{ds} + L_m (i_{ds} + i_{dr}) \quad (11)$$

$$\lambda_{qs} = Ll_s i_{qs} + L_m (i_{qs} + i_{qr}) \quad (12)$$

$$\lambda_{xs} = Ll_s i_{xs} \quad (13)$$

$$\lambda_{ys} = Ll_s i_{ys} \quad (14)$$

$$\lambda_{os1} = Ll_s i_{os1} \quad (15)$$

$$\lambda_{os2} = Ll_s i_{os2} \quad (16)$$

$$\lambda_{dr} = Ll_r i_{dr} + L_m (i_{ds} + i_{dr}) \quad (17)$$

$$\lambda_{qr} = Ll_r i_{qr} + L_m (i_{qs} + i_{qr}) \quad (18)$$

$$\lambda_{md} = L_m (i_{ds} + i_{dr}) \quad (19)$$

$$\lambda_{mq} = L_m (i_{qs} + i_{qr}) \quad (20)$$

where λ is the flux leakage, L_m the magnetizing inductance and Ll_s and Ll_r are the stator and rotor inductance.

The mechanical equations of the machine are given as;

$$T_{em} = \frac{6}{2} \frac{P}{2} (\lambda_{ds} i_{qs} - \lambda_{qs} i_{ds}) \quad (21)$$

$$\omega_r = \int \left(\left(\frac{P}{2} \right) \left(\frac{1}{J} \right) (T_{em} - T_{load}) \right) dt \quad (22)$$

where J is the moment of inertia, T_{em} , the electromagnetic torque, ω_r the speed and T_{load} is the load torque.

The real and reactive powers are also given as;

$$P = 3 (V_{ds} I_{ds} + V_{qs} I_{qs}) \quad (23)$$

$$Q = V_{ds} I_{qs} - V_{qs} I_{ds} \quad (24)$$

Finally the power factor is expressed as:

$$\cos \theta = \frac{P}{S} = \frac{P}{P + jQ} \quad (25)$$

The transformation matrix of the six phase stator voltages are expressed in (26) by setting $\theta = 0$ [11] yielding

$$K_s = \frac{1}{3} \begin{bmatrix} 1 & \frac{1}{2} & -\frac{1}{2} & -1 & -\frac{1}{2} & \frac{1}{2} \\ 0 & \frac{\sqrt{3}}{2} & \frac{\sqrt{3}}{2} & 0 & -\frac{\sqrt{3}}{2} & -\frac{\sqrt{3}}{2} \\ 1 & -\frac{1}{2} & -\frac{1}{2} & 1 & -\frac{1}{2} & -\frac{1}{2} \\ 0 & \frac{\sqrt{3}}{2} & -\frac{\sqrt{3}}{2} & 0 & \frac{\sqrt{3}}{2} & -\frac{\sqrt{3}}{2} \\ \frac{1}{2} & \frac{1}{2} & \frac{1}{2} & \frac{1}{2} & \frac{1}{2} & \frac{1}{2} \\ \frac{1}{2} & -\frac{1}{2} & \frac{1}{2} & -\frac{1}{2} & \frac{1}{2} & -\frac{1}{2} \end{bmatrix} \quad (26)$$

One remarkable property of the matrix above is that its inverse equals its transpose. That is

$$K_s^{-1} = K_s^T \quad (27)$$

where T is the transpose.

III. VALIDATION OF THE GLOBAL MODEL

From the previous equations it is possible, using Matlab-Simulink®, to compute the transient and steady state behavior of the machine in terms of torque, speed, current, etc. The machine specifications are summarized in Table I. Also, to be able to compare the obtained theoretical results to experimental ones, the experimental setup described in Fig. 2 was realized. The set up consists of a six-phase induction machine supplied via a six phase generator and coupled to a dynamometer. An oscilloscope Tektronix THS 720A is used to record the signals in play.

TABLE I
SIMULATION PARAMETERS

Symbol	Description	Value
R_s	Stator resistance	21 Ω
R_r	Rotor resistance	11.033 Ω
L_{ls}	Stator leakage inductances	0.02603 H
L_{lr}	Rotor leakage inductances	0.02603 H
L_m	Magnetizing inductance	3.047 H
J	Moment of inertia	0.00702 Kg m^2
V	Voltage	169.423 V
P	Power	1 Kw
f	frequency	50 Hz

The procedure performed for the theoretical and experimental tests considers the scenario whereby firstly, all phases are connected to the supply voltage, secondly, one of the phases is opened and lastly one of the phases is short-circuited.

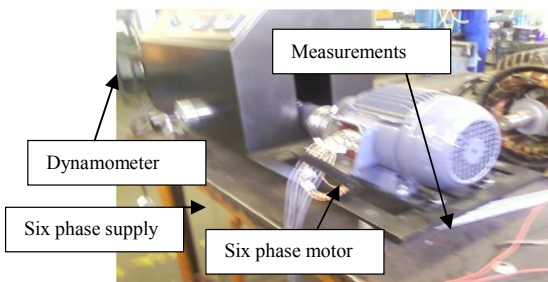


Fig. 2 Experimental set-up

Also for the test performed under a load condition, the machine had been loaded to approximately 125% of the rated torque identified as the point at which the machine breaks down.

The simulation and experimental results are given in Fig. 3. The good agreement, shown by the curves, between theoretical and experimental results tends to validate the model.

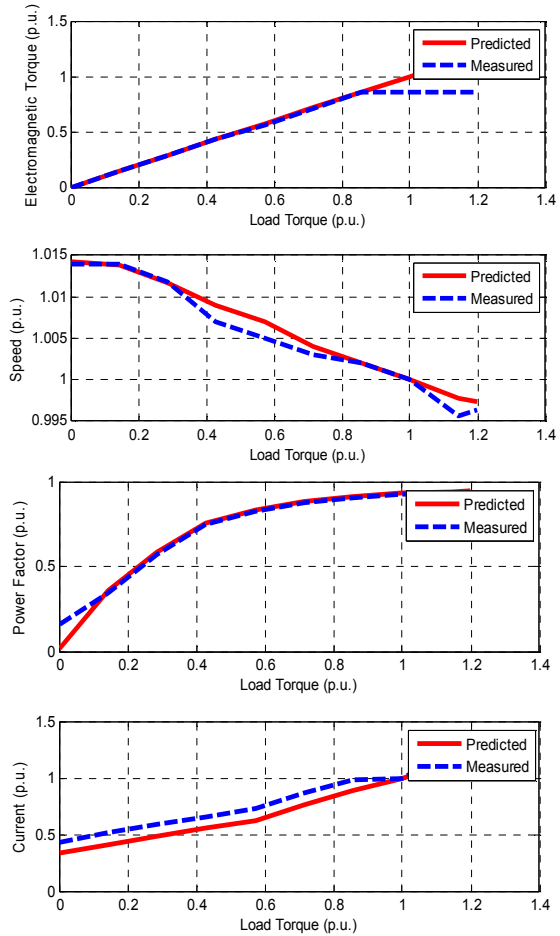


Fig. 3 Torque, speed, power factor and current as function of load

IV. SIMULATION OF A HEALTHY MACHINE

The dynamic simulation of the machine is done in the arbitrary reference frame. The analysis is carried out when all the phases are connected. These are for two scenarios: firstly, at no load and secondly at rated load. Under such conditions the obtained electromagnetic torque, speed and stator currents are as shown in Fig. 4 and Fig. 5.

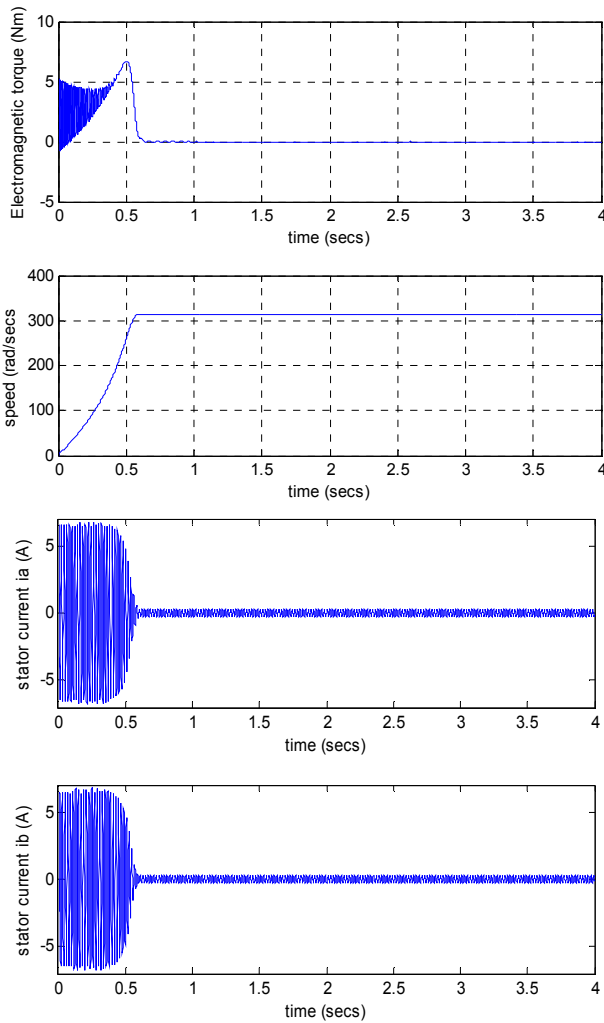


Fig. 4 Theoretical electromagnetic torque, speed, stator current of phase *a* and phase *b* with all phases connected, no load condition

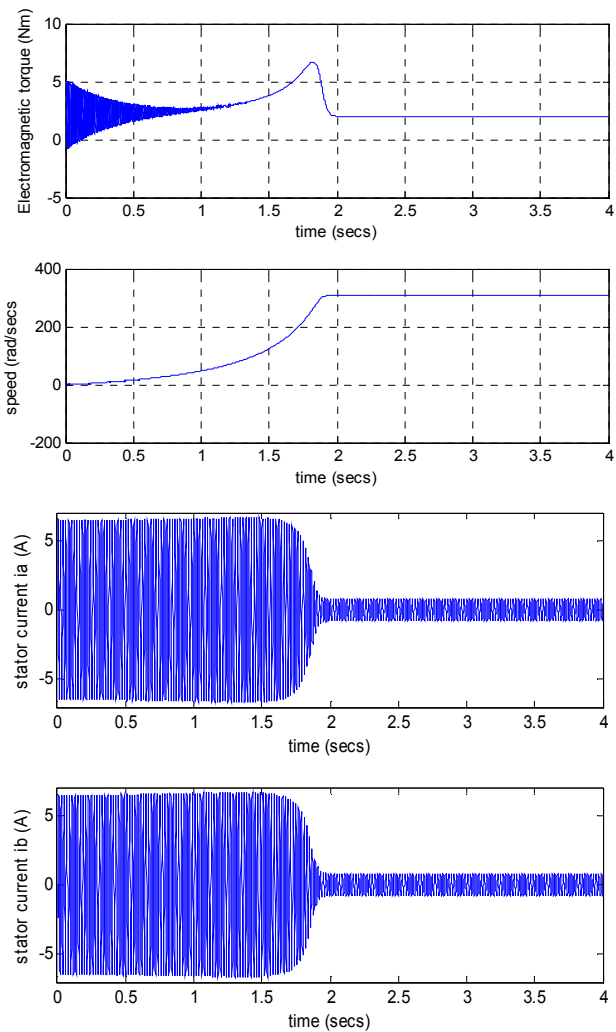


Fig. 5 Theoretical electromagnetic torque, speed, stator current of phase *a* and phase *b* with all phases connected, loaded machine

It can be observed that the response of the machine to changes in loading remains the same in parameters magnitude. However, the loaded machine takes longer to settle in steady state compared to the unloaded one (ratio of approximately 1:2 times). Also a torque of 1.8 Nm is produced by the loaded machine in steady state against no torque in unloaded condition as expected.

V. FAULT ANALYSES

To analyze the unhealthy machine two types of fault are distinguished. Firstly the open circuit faults are simulated and then the short circuit faults, both in unload and load conditions.

A. Open Circuit Fault Analysis

Starting the investigation with open phase analysis the machine is modeled for ease of referral in the stationery reference frame where $\omega = 0$. The open circuit fault can be simulated by simply assuming that the current ceases to flow

after a normal current zero. Which zero value is maintained by replacing in simulation the source voltage with open circuit voltage [7][5].

The star connected phases of the stator currents without the neutral connection are expressed as:

$$I_{as} + I_{bs} + I_{cs} + I_{xs} + I_{ys} + I_{zs} = 0 \quad (28)$$

The phase voltages between the neutral points may be given as:

$$V_{sg} = \frac{1}{6} \sum_{v=a}^z V_{is} - V_{ig} \quad (29)$$

When stator current phase a is opened,

$$V_{sg} = \frac{1}{5} \sum_{v=b}^z V_{is} - V_{ig} \quad (30)$$

Since the machine is connected in star, I_{os1} and $I_{os2} = 0$.

From (28), the phase *a* current may be expressed as:

$$I_{as} = I_{ds} + I_{xs} \quad (31)$$

From (31), when $I_{as} = 0$, $I_{ds} = -I_{xs}$.

The open circuit voltage is expressed as:

$$V_{as} = V_{ds} + V_{xs} \quad (32)$$

Back-substituting $I_{ds} = -I_{xs}$ into (3) and (5) and using (13), (17) gives,

$$V_{dcs} = r_s \left(\frac{\lambda_{dcs}}{l_{ls}} \right) + \frac{d}{dt} \lambda_{dcs} \quad (33)$$

$$V_{ds} = -r_s \frac{\lambda_{xs}}{l_{ls}} - \frac{L_s}{L_{lr}} \frac{d}{dt} \lambda_{xs} + \frac{L_m}{L_r} \frac{d}{dt} \left(\lambda_{dr} + \frac{L_m}{L_{ls}} \lambda_{xs} \right) \quad (34)$$

where $L_s = L_{ls} + L_{lr}$ and $L_r = L_{lr} + L_m$

It is to notice that replacing *d*-axis current with *x*-axis current in [9] Miranda et al similarly obtained the expression giving V_{ds} as a function of currents which they directly implemented for the study they conducted. In our case we rather use the other form of the equation yielding V_{ds} as a function of flux linkages.

The torque and power derived may be expressed as:

$$T_{em} = \frac{6}{2} \frac{P}{2} (\lambda_{ds} i_{qs} + \lambda_{qs} i_{xs}) \quad (35)$$

$$P = 3 (V_{ds} I_{xs} + V_{qs} I_{qs}) \quad (36)$$

$$Q = V_{ds} I_{qs} - V_{qs} I_{xs} \quad (37)$$

Implementing the equations above enables the machine behavior analysis under no load and load conditions. The fault was created while the machine had been running from standstill for 1.5 seconds and the obtained results are shown in Fig. 6 and Fig. 7.

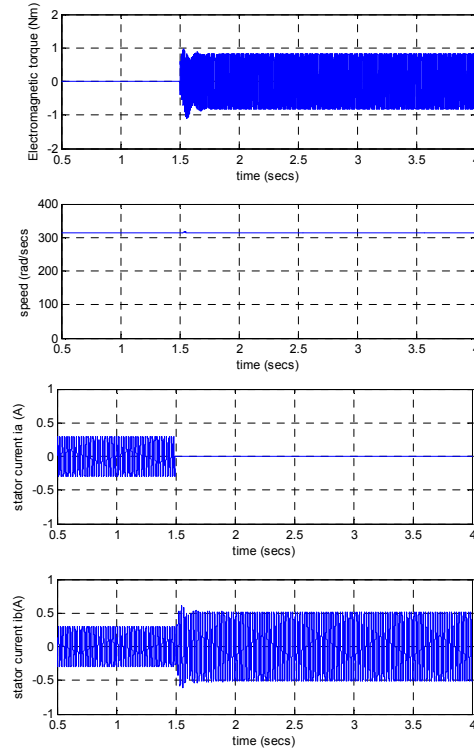


Fig. 6 Electromagnetic torque, speed, stator current of phase *a* and phase *b* with one phase opened. o load condition

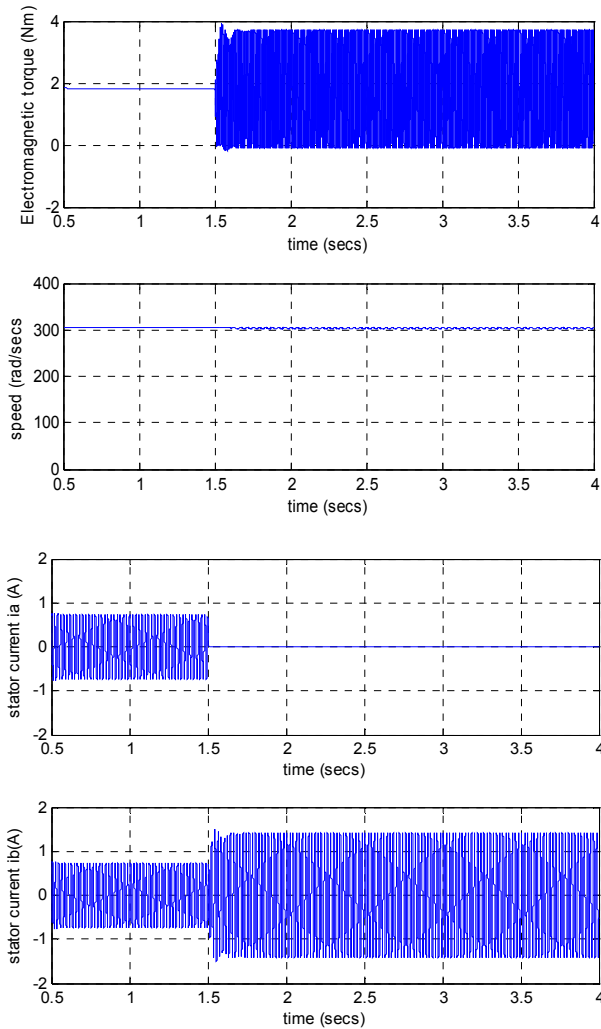


Fig. 7 Electromagnetic torque, speed, stator current of phase *a* and phase *b* with one phase opened, loaded machine

From the fault occurrence time the current in the faulty phase *a* is zero as expected and the amplitude of the oscillations in phase *b* raised to reach a constant value. That is affecting the torque subject in turn to oscillations around respectively 0 and 1.8 Nm developed in healthy conditions at no load and full load. That is true especially in loaded conditions where the amplitude of those torque oscillations is nearly twice that observed in no load conditions. No significant change is observed in speed. Most remarkably, unlike in [7] where the phase is briefly opened, the attained amplitude of the oscillations is not varying despite the presence of a fault rather permanent that is uncleared.

B. Short Circuit Fault Analysis

In this section the faulty situation is examined in which a short circuit that is a common accident, able to tear windings apart, occurs. The example may help to better understand the operational behavior of the machine. For that instance, we

basically consider that the star connected phases of the stator voltages without the neutral connection may be expressed as:

$$V_{as} + V_{bs} + V_{cs} + V_{xs} + V_{ys} + V_{zs} = 0 \quad (38)$$

If in the preceding instance whereby the open phase fault is analyzed, the sum of currents is taken equal to zero in (28), this time the different currents have been replaced by voltages yielding (38).

For the theoretical analysis of short circuit, a fault was created at 1.5 seconds after the machine started from standstill.

The results, shown in Fig. 8 and 9 are the obtained electromagnetic torque, speed and stator currents.

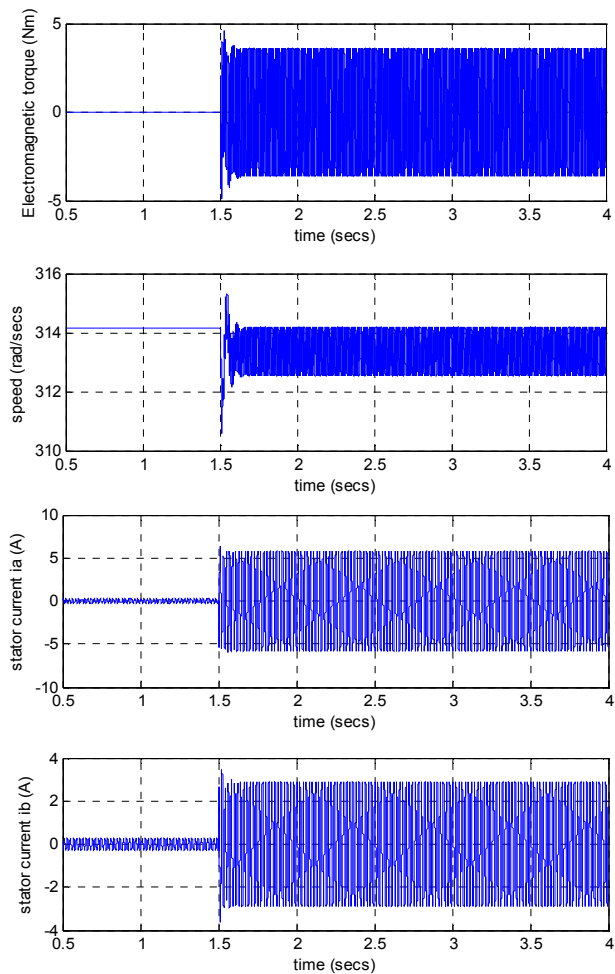


Fig. 8 Electromagnetic torque, speed, stator current of phase *a* and phase *b* with one phase opened, machine unloaded

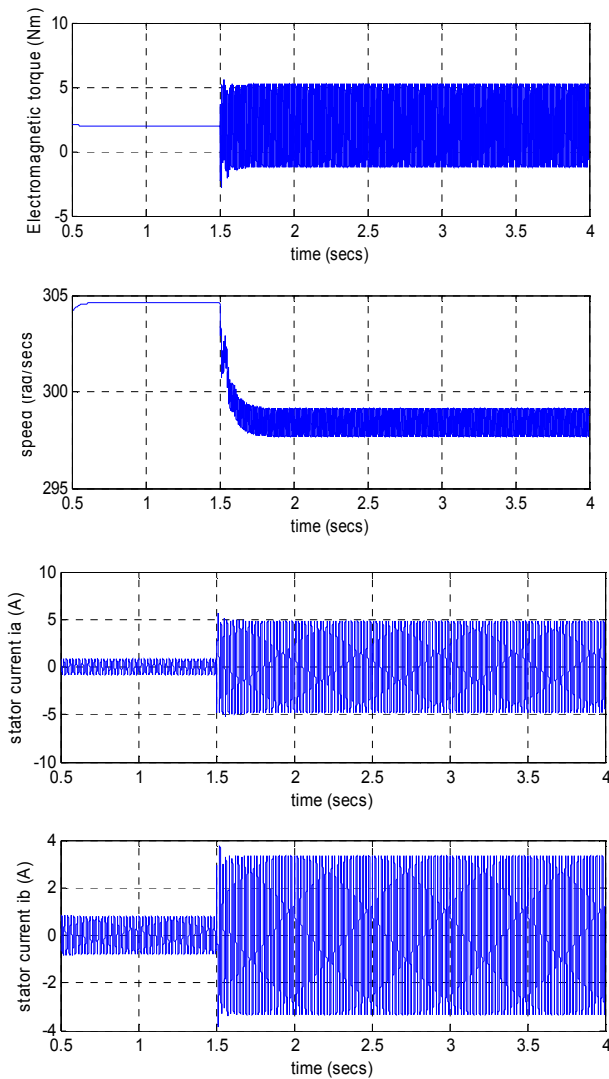


Fig. 9 Electromagnetic torque, speed, stator current of phase *a* and phase *b* with one phase opened, machine loaded

In this instance currents in both phase *a* and phase *b* are subject to oscillations having the same impact on the torque as in the open circuit fault but simply the amplitude of the oscillations appearing is slightly greater. Conversely, the speed drops slightly and oscillates around a certain average value.

From the effects of the short circuit simulated above on the torque and speed it is apparent that we are in presence of the most severe fault. However the machine performance is not critically affected.

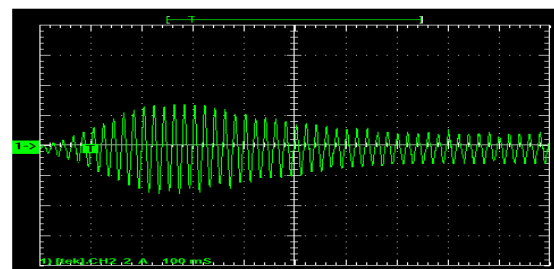
VI. EXPERIMENTAL RESULTS

As a precaution, the machine transients as well as power, stator voltage and current wave shapes were recorded using the Tektronix THS 720A. The signals mentioned above are shown in Fig. 10 (a), (b), and (c). To observe the current in

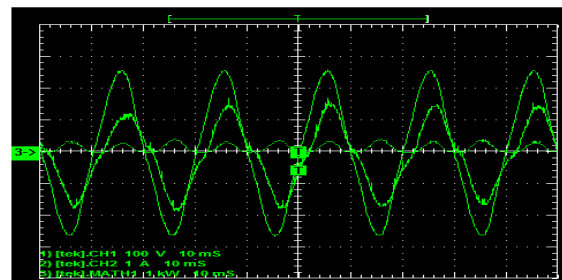
one of the phases during the transients, the measurements are made when all phases are connected, first and then in single phasing. Finally, the instantaneous voltage, current and power wave shapes were recorded with all the phases connected.

A straight comparison between the wave shapes displayed in Fig. 10 and the corresponding ones from simulation is not possible at least since there is no scale available for the figure. Nevertheless it is apparent that transient and steady state can easily be identified on the screen making a clear difference between a healthy (with decaying oscillations in Fig. 10 (a).) and a faulty machine as in simulation.

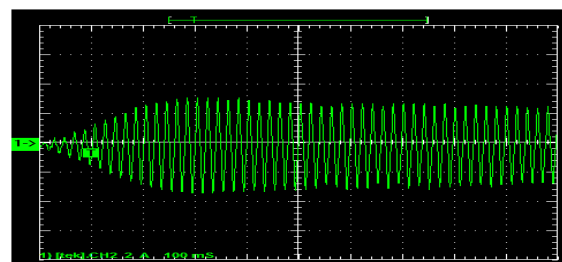
The small angle difference between voltage and current from the machine having its six phases connected in Fig. 10 (b) gives an idea of high power factor and consequently assesses that the machine is indeed healthy.



(a) Transients starting current in phase *A* when all six-phase are connected



(b) Phase voltage, phase current and power for phase *A* when all six-phase are connected



(c) Transient characteristics of phase *b* when phase *a* was opened

Fig. 10 Experimental recordings

VII. CONCLUSION

In this paper the dynamic and transient performance of a six-phase induction machine with faults on the stator phases has been analyzed. The model is built by using the $abcxyz$ to $\alpha - \beta$ transformation in the arbitrary rotating reference frame. Also a stationary reference frame is used for the fault analysis. The machine is first simulated with all six-stator phases connected to the AC supply separately unloaded and loaded conditions and then is simulated with one of the stator phases open or short circuited. The result obtained showed that in both cases the machine is able to produce the starting torque. However it is observed that the torque produced of the healthy machine is greater in magnitude and produces fewer oscillations than the machine with an open-circuit fault at the stator phase. It is recommended that de-rating of the machine under faulty conditions be taken into consideration as it can be observed that high increase of currents under faulty condition can cause overheat which can damage the windings.

Further research is on-going. Future work includes:

- a. the analytical analysis of the machine taking into consideration the permanence effects and
- b. The Finite Element Analysis of the experimental machine.

REFERENCES

- [1] A. Yong-le, K. J. Maarten and A. D. Le Roux, "Novel Direct Flux and Direct Torque Control of Six-Phase Induction Machine With Nearly Square Air-Gap Flux Density", IEEE Transactions on Industry Applications, Vol. 43, no. 6, November-December 2007.
- [2] T. A. Lipo, "A d-q model for six-phase induction machines", in Proc. Int. Conf. Electrical Machines, vol.2, pp. 860-867, 1980.
- [3] G. K. Singh, "Multi-phase induction machine drive research" – a survey, Electric Power Systems Research, vol. 61, no. 2, pp. 139-147, 2002.
- [4] J. Apsley, S. Williamson, "Analysis of Multiphase Induction Machines with Winding Faults", IEEE Transactions on Industry Applications, VOL. 42, NO. 2 March-April 2006.
- [5] P. C. Krause and C. H. Thomas, "Simulation of Symmetrical Induction Machinery", IEEE Trans. on Power Apparatus and Systems, Vol. PAS-84, No. 4, pp. 1038–1049, 1965.
- [6] M. O. Chee, "Dynamic Simulations of Induction Machine using Matlab/Simulink", School Of Electrical and Computer engineering, Purdue University, West Lafayette, Prentice hall, 1998.
- [7] G. K. Singh, P. Vinay, "Analysis of a Multiphase Induction Machine under Fault Condition in a Phase-Redundant A.C. Drive System". Electric Power Components and Systems, 28: 6, 577 — 590
- [8] Y. Zhao and T. A. Lipo, "Modelling and Control of Multi-Phase Induction Machine with Structural Unbalance", IEEE Transactions on Energy Conversion, Vol. 11, No. 3, September 1996.
- [9] R. S. Miranda, C. B. Jacobina, A. M. N. Lima, "Modelling and Analysis of Six-Phase Induction Machine under Fault Condition", Power Electronics Conference, 27 September-1 October 2009, COBEP '09, Brazilian.
- [10] P. C. Krause, O. Wasynczuk, S. D. Sudhoff, "Analysis of Electric Machinery and Drive Systems", Second Edition, IEEE Press 2002.
- [11] E. Levi, Recent Developments in High "Performance Variable-Speed Multiphase" Induction Motor Drives, IEEE Trans. on Energy Conversion, Vol. EC-11, No. 3, pp. 570–577, 2006.
- [12] T. Wildi, "Electrical Machines, Drives, and Power Systems", Sixth Edition, International Edition, Pearson Prentice Hall, 2004.
- [13] J. R. Kianinezhad, B. N. Mobarakeh, L. Baghli, F. Betin, and G. Capolino, "Modeling and Control of Six-Phase Symmetrical Induction Machine Under Fault Condition Due to Open Phases," IEEE Trans. Ind.Electron.VOL.55, Issue 5, pp 1966-1977, May 2008.